University of Nebraska - Lincoln
DigitalCommons@University of Nebraska - Lincoln

Ralph Skomski Publications | Research Papers in Physics and Astronomy

June 1998

# Hydrogen in $R_2Fe_{17}$ intermetallic compounds: Structural, thermodynamic, and magnetic properties

S. Wirth
*Trinity College, Dublin, Ireland*

Ralph Skomski
*University of Nebraska-Lincoln*, rskomski2@unl.edu

J.M.D. Coey
*Trinity College, Dublin, Ireland*

Follow this and additional works at: https://digitalcommons.unl.edu/physicsskomski

 Part of the Physics Commons

Wirth, S.; Skomski, Ralph; and Coey, J.M.D., "Hydrogen in $R_2Fe_{17}$ intermetallic compounds: Structural, thermodynamic, and magnetic properties" (1998). *Ralph Skomski Publications*. 26.
https://digitalcommons.unl.edu/physicsskomski/26

This Article is brought to you for free and open access by the Research Papers in Physics and Astronomy at DigitalCommons@University of Nebraska - Lincoln. It has been accepted for inclusion in Ralph Skomski Publications by an authorized administrator of DigitalCommons@University of Nebraska - Lincoln.

# Hydrogen in $R_2Fe_{17}$ intermetallic compounds: Structural, thermodynamic, and magnetic properties

S. Wirth,* R. Skomski,† and J. M. D. Coey
*Department of Physics, Trinity College, Dublin 2, Ireland*
(Received 14 June 1996; revised manuscript received 26 August 1996)

The absorption and diffusion behavior of hydrogen in iron-rich rare-earth intermetallics of the type $R_2Fe_{17}$ ($R$=Y, Sm, Gd) and the resulting changes of their magnetic properties are investigated. Intermediate hydrogen concentration indicate the solid-solution character of the hydrides. From equilibrium and nonequilibrium absorption experiments net reaction energies, bulk diffusion constants, and surface barrier energies for $Sm_2Fe_{17}$ are determined and discussed. The low-temperature quantum diffusion is discussed for the hydride and the corresponding nitride. The interstitial modification changes drastically the crystalline electric field in the rare-earth intermetallics. For $Sm_2Fe_{17}H_4$ the crystalline electric-field parameter $A_{20}$=110 $Ka_0^{-2}$ is estimated from the anisotropy constants $K_1$ and $K_2$. [S0163-1829(97)00310-X]

## I. INTRODUCTION

It has long been known that certain metals are able to absorb large quantities of gases.[1] Among them iron-rich intermetallic compounds with rare-earth elements ($R$) have attracted special interest.[2] A famous example is hydrogen in $LaNi_5$, where loadings of up to $LaNi_5H_{6.7}$ have been observed.[3]

However, the importance of interstitially modified rare-earth intermetallics is not only due to their hydrogen storage properties, but also to the significant changes in magnetic properties. Hydrogen in $Sm_2Fe_{17}$ increases[4] the Curie temperature by about 140 K. A further enhancement of Curie temperature can be obtained[5] substituting some iron by cobalt (e.g., $T_c$=607 K for $Nd_2Fe_{15}Co_2H_x$, $x\sim2.5$). In the case of nitrogen in $Sm_2Fe_{17}$, the Curie temperature increase is about 360 K, and the nitride $Sm_2Fe_{17}N_{3-\delta}$ is a promising permanent magnet material.[6]

In the rhombohedral $Sm_2Fe_{17}$ structure there are two different interstitial sites which are likely to accommodate interstitial atoms: three large octahedral sites ($9e$) and six smaller tetrahedrals ($18g$). Hydrogen occupies both $9e$ and $18g$ sites, but the $18g$ occupancy has been reported to be restricted to two hydrogen atoms per formula units, probably in dumbbell configuration.[7,8] This behavior reflects a repulsive short-range interaction between different hydrogen atoms and gives rise to the general rule, that the H distances not be shorter than 2.1 Å (cf., e.g., Ref. 9 and references therein).

Molecular gases in metals typically dissociate at the metal surface and the atoms occupy octahedral and tetrahedral interstitial sites.[10] A key question is whether the interstitially modified material represents a new compound or simply a gas-solid solution. Hydrides of 1–5 intermetallics usually show an $\alpha-\beta$ phase transition above room temperature at moderate pressure.[11] Above the transition temperature $T_c(\alpha-\beta)$ the hydride represents a gas-solid solution with intermediate hydrogen content. Below $T_c(\alpha-\beta)$ phase segregation occurs and the hydrogen-rich ($\beta$) phase is separated from the hydrogen-poor ($\alpha$) solid solution by a solubility gap.

The $\alpha-\beta$ phase transition is evidence of an attractive interaction between interstitial atoms, which has its origin in the elastic deformation of the lattice around the interstitials.[12] This interaction and hence $T_c(\alpha-\beta)$ increase with the concentration of interstitial sites in question and with the lattice expansion $v_0$ per interstitial atom, which is typically 2.9 Å$^3$ for hydrogen in metals.[13]

Beside Curie temperature and saturation magnetization, the magnetic anisotropy of the intermetallic compounds is also influenced by interstitial modification.[6,14–18] However, unlike nitrogen and carbon, the modification of the crystal electric field by hydrogen is rather small and no change from easy-plane to easy-axis anisotropy occurs for the $Sm_2Fe_{17}$-hydrogen system.[4]

Generally, hydrogen absorption is of special interest because of the higher solubility and mobility of the hydrogen atoms in metals compared with nitrogen and carbon. Equilibrium can be established readily. Here we investigate solubility and diffusion of hydrogen in 2–17 compounds and the influence of hydrogen on the crystalline electric field in $R_2Fe_{17}$ compounds. Some structural and magnetic properties of the 2–17 hydrides have recently been discussed by Fruchart *et al.*[19] It should be noted that our results for solubility and diffusion may be applied to other iron-rich rare-earth intermetallics.

## II. HYDROGEN UPTAKE OF METALS

### A. Hydrogen absorption and desorption behavior

A simple way to investigate the absorption and desorption of hydrogen is the observation of the gas pressure in a fixed volume at constant heating (cooling) rate. This method yields rapid results and can be used to get an illustrative idea of the absorption/desorption process. The experiments were carried out in a thermopiezic analyzer[20] (TPA) where the temperature dependence of the gas pressure is measured in a closed volume containing the material to be hydrogenated. Intermetallics can be prepared with various hydrogen contents by controlling the temperature $T$ or pressure $P$ in the sample

 © 1997 The American Physical Society

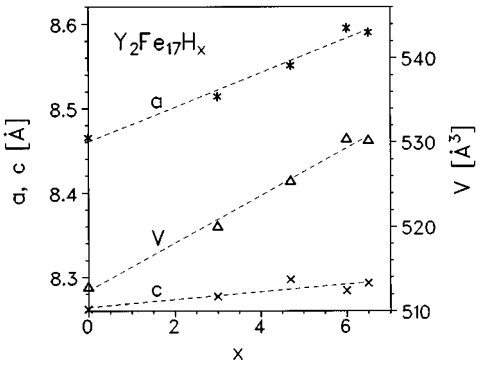


FIG. 1. Lattice expansion for hydrogenated $Y_2Fe_{17}H_x$.

space. Hydrogen contents are derived from the pressure change before and after the reaction, measured at ambient temperature.

The $R_2Fe_{17}$ alloys with $R$=Y, Sm, Gd were prepared by arc melting the $3N$ pure elements in an arc furnace, and annealing in vacuum at 1000 °C. Powdered material $\leqslant 40$ $\mu$m was used for the hydrogenation experiments. It was noted that $R_2Fe_{17}$ compounds of the light rare earths in particular will absorb hydrogen if left in ambient air.[21] This may be associated with a layer of water on the surface of the powder particles.

The $R_2Fe_{17}$ intermetallics of Sm and Gd crystallize in the rhombohedral $Th_2Zn_{17}$ structure whereas that of Y is found to form the hexagonal $Th_2Ni_{17}$ structure. The lattice parameter for $Y_2Fe_{17}H_x$ with $x$ ranging from 0 to 6.5 are shown in Fig. 1. The volume increase of 2.7 Å$^3$ per hydrogen atom is in agreement with the value reported elsewhere[19] and confirms the complete absorption of the hydrogen onto interstitial sites. However, the maximum hydrogen uptake of $x \approx 3.4$ given in Ref. 19 is much less than that shown in Fig. 1 which can be ascribed to different conditions during hydrogenation [$T$ and $P$, cf. Eq. (2)]. A typical result for the hydrogen uptake obtained for $Y_2Fe_{17}$ heated at a constant rate of 10 K min$^{-1}$ in the TPA is shown in Fig. 2. From the pressure decrease can be seen that the hydrogen absorption starts at 200 °C (stage I), which is a typical value in $R_2Fe_{17}$ powder. With increasing temperature the occupation probability (concentration $x$) decreases as the hydrogen desorbs. The second decrease in pressure (stage II) is due to the decomposition ($RH_{2-\varepsilon}+\alpha$-Fe) of the hydrogen-containing compound.[4] In the case of $Sm_2Fe_{17}$ or $Nd_2Fe_{14}B$, this decomposition is used for grain refinement in the HDDR process of magnet manufacture as developed by Takeshita.[22]

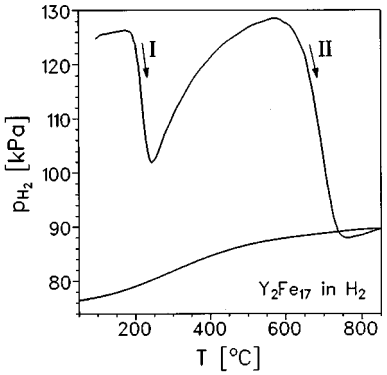


FIG. 2. Measured TPA trace of $Y_2Fe_{17}$ for a heating rate 10 K min$^{-1}$. The absorption (I) and disproportionation (II) states are marked.

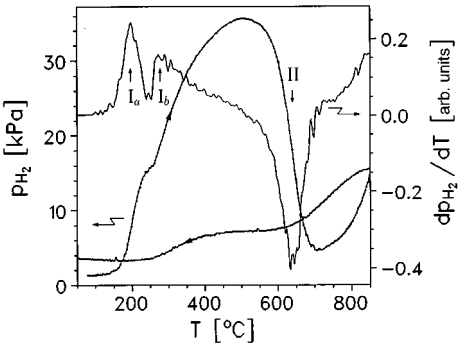


FIG. 3. TPA trace and differential plot $dp/dT$ of $Gd_2Fe_{17}H_{2.0}$ heated in vacuum. The two outgasing modes corresponding to the different binding energies of tetrahedral ($I_a$) and octahedral ($I_b$) sites are visible.

If $R_2Fe_{17}H_x$ is treated in vacuum the differential analysis clearly shows two outgassing modes (example $Gd_2Fe_{17}H_{2.0}$ in Fig. 3). This behavior may be attributed to assuming different binding energies for different interstitial sites, presumably the tetrahedral and octahedral sites. After partial degassing of the compound, the pressure trace measured in the TPA again exhibits two desorption features $I_a$ and $I_b$, indicating that an equilibrium population of hydrogen in weakly and strongly bound sites is established rapidly.

Measurements at constant heating rate mix equilibrium and nonequilibrium properties, and it is difficult to determine parameters like diffusion constants or binding energies from constant heating rate experiments. By heating of $R_2Fe_{17}D_x$ in vacuum and following neutron-diffraction investigation, Isnard *et al.*[7] have examined the behavior of concentration of the different octahedral and tetrahedral interstitials.

### B. Gas-solid solution

The solubility of hydrogen in metals depends mainly on three factors: (i) the electronic interaction between interstitial atoms and metal lattice, (ii) the entropy difference between gaseous and interstitial hydrogen, and (iii) the interatomic interaction of the hydrogen atoms in the lattice. If the net reaction energy (absorption energy) $U_0$ is negative, a high hydrogen concentration in the metal is favorable. On the other hand, thermal activation tries to remove the atoms from the lattice again, and in the high-temperature limit ($k_BT \gg U_0$) the solubility is very low, and it is mainly determined by the entropy of the solid solution.

The interatomic interaction is mainly due to long-range elastic strain. For isolated grains it is attractive[12] and leads to phase segregation for $T < T_c$, where $T_c$ is the critical temperature of the phase transition. $T_c$ depends explicitly on the boundary conditions. As an example, in Ref. 23 a shape dependence of $T_c$ in Nb samples was reported. It is possible to observe the miscibility gap below $T_c$ by x-ray-diffraction line-shape analysis.[24,25] The x-ray-diffraction lines split into two separate lines, whereas above $T_c$ single intermediate

peaks indicate intermediate lattice parameters. Hydrogen in $R_2Fe_{17}$ at room temperature does not yield any line splitting, so the $R_2Fe_{17}H_x$ system can be regarded as a more or less ideal solution. This corresponds to the behavior of the nitrided system $Sm_2Fe_{17}N_x$, where a gas-solid solution has been deduced from different investigations.[25–27] The reason for this behavior (hydrogen-metal systems are often treated as nearly two-phase[2]) is the low mean concentration of interstitial atoms [maximum $6/(17+2)=0.31$] compared to $LaNi_5$ [maximum $6/(5+1)=1.0$]. This means that there is a lower elastic strain, and thus a lower critical temperature in the 2:17 system.

In the framework of a continuum theory, $T_c$ can be estimated[28,29]

$$k_B T_c \approx K\left(\frac{\Delta V}{V}\right)^2 \frac{V}{N_i}, \tag{1}$$

where $K$ is the bulk modulus, $\Delta V/V$ is the relative lattice expansion due to interstitial modification, and $N_i$ is the number of interstitial sites in the volume $V$. In this consideration, changes in the electronic configuration of the host system by the hydrogen uptake has been neglected.[30] Using the value $K=106$ GPa which should be a good approximation for iron-rich rare-earth intermetallics,[31] $T_c \approx 387$ K can be estimated. Although this is only a crude estimate it justifies considering the material as single phase in the following.

In the ideal solution case the occupation numbers (interstitial concentrations) can be calculated by a lattice gas model[25,32] which yields the equilibrium hydrogen content $x$ in $R_2Fe_{17}H_x$

$$x=\frac{3}{1+\sqrt{P_0/P}\exp(U_{\rm oct}/k_BT)}+\frac{2}{1+\sqrt{P_0/P}\exp(U_{\rm tet}/k_BT)}. \tag{2}$$

$U_{\rm oct}$ and $U_{\rm tet}$ are the net reaction energies (solution energies) for octahedral and for tetrahedral occupation, respectively, and $P_0$ is a constant which describes the entropy loss during reaction.[10] For low hydrogen concentration, i.e., at high temperature, Eq. (2) reduces to the well-known Sieverts law.[33] With fixed $P_0 \approx 2\times10^6$ bar we obtain

$$U_{\rm oct}=-26\ (\pm 4)\ \ {\rm kJ\ mole^{-1}},$$

$$U_{\rm tet}=-18\ (\pm 10)\ \ {\rm kJ\ mole^{-1}},$$

whereby it was assumed that for high temperatures the octahedral interstitials are occupied only. Note that the given value of $U_{\rm tet}$ is a crude estimation from the temperature dependence of hydrogen pressure during heat treatment of hydrogenated material under vacuum.

### III. HYDROGEN DIFFUSION

The propagation of hydrogen in the bulk of a rare-earth intermetallic is diffusion controlled.[34] In general, the diffusion of hydrogen can be described in a mean-field approximation by[35]

$$D_{\rm MF}=D\left[1-4c(1-c)\frac{T_c}{T}\right], \tag{3}$$

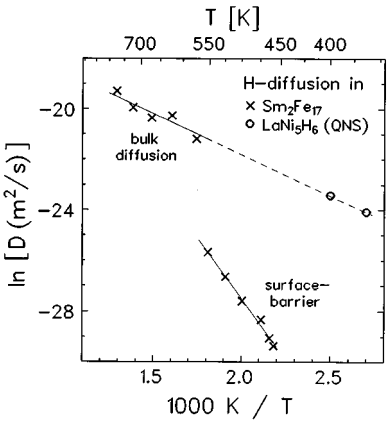


FIG. 4. Arrhenius plot for the measured hydrides; the decrease of absorption by the surface barrier is clearly recognizable; the $LaNi_5H_6$ data were obtained by quasielastic neutron scattering (Ref. 34).

where $c$ is the fractional concentration of H atoms on the interstitial sites in the intermetallic compound ($0 \leqslant c \leqslant 1$) and $D_{\rm MF}$ is the resulting diffusivity which is concentration dependent. The diffusion constant $D$ is controlled by the dominant diffusion mechanism at the temperature considered and hence the diffusion mechanism itself is not influenced by the value of $T_c$. For temperatures $T>T_c$ the diffusivity $D_{\rm MF}$ is positive and spatial differences of $c$ will be smoothed out with time. It should be noted that for the case of interest here, where $T>T_c$ and thermal activation is predominant the temperature dependence of $D_{\rm MF}$ is mainly given via $D$ [exponential law Eq. (13)] and—according to a general rule—the $1/T$ dependence [brackets in Eq. (3)] cannot be separated experimentally but leads to a small correction of the diffusion constant. Henceforth, we will not distinguish between $D_{\rm MF}$ and $D$. For $T<T_c$ and $\frac{1}{2}(1-\sqrt{1-T/T_c}) < c < \frac{1}{2}(1+\sqrt{1-T/T_c})$ *the diffusivity* $D_{\rm MF}$ *is negative and a phase segregation occurs*.

The absorption rate of hydrogen at about 200 °C is much lower than expected from the bulk diffusion constant of the similar $LaNi_5H_6$ system[34] (Fig. 4). This difference can be explained by the experimental conditions. In the TPA, the hydrogen molecules have to dissociate and to penetrate the surface of the particles to be hydrogenated (in contrast to the neutron measurements of Ref. 34). Therefore a surface barrier energy $U_s$ arises, as illustrated in Fig. 5. If the particle flux $j_s$ through the surface barrier is smaller than the possible diffusion flux $j_d$ under the surface layer the reaction rate is

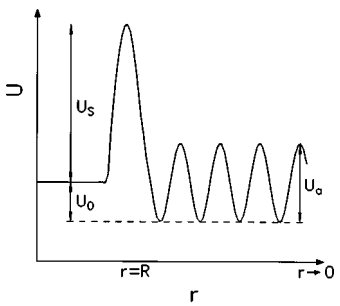


FIG. 5. Definition of the used energies.

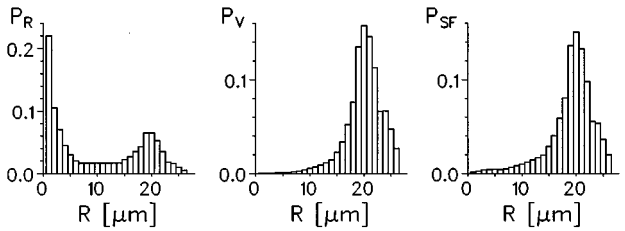


FIG. 6. Particle size distribution ($P_R$) and corresponding volume ($P_V$) and surface area distribution ($P_{SF}$) of the powder used for investigation of the surface barrier.

surface controlled. In the opposite case, the surface barrier can be neglected and the absorption of the hydrogen atoms in the bulk material is controlled by the bulk diffusion constant. The surface and bulk controlled diffusion regimes may be distinguished in experiments where the gas pressure dependence on time is measured at fixed temperature.

### A. Surface controlled reaction

To realize this mode, a high diffusion flux must be assured. Considering the diffusion equation for spherical grains (site-blocking effects do not yield any concentration dependence of the diffusion constant[35])

$$\frac{\partial c}{\partial t} = D\left(\frac{\partial^2 c}{\partial r^2} + \frac{2}{r}\frac{\partial c}{\partial r}\right) \tag{4}$$

with the boundary condition

$$\left.\frac{\partial c}{\partial r}\right|_R = \frac{j_s}{D}, \tag{5}$$

a solution in the small $j_s$ limit is given by

$$c(r,t) = \frac{j_s}{D}\left(\frac{r^2}{2R} + \frac{3Dt}{R} - \frac{3R}{10}\right). \tag{6}$$

This solution is valid for the initial stage of hydrogenation only. In order to obtain a reasonable surface flux rate the surface-volume ratio should be chosen high. Here grains with a mean particle diameter of about 40 $\mu$m have been used. The particle size distribution as obtained from optical micrographs and the corresponding particle surface area and volume distributions are shown in Fig. 6.

The flux through the surface barrier $U_s$ can be described by

$$j_s = j_0 \exp(-U_s/k_BT), \tag{7}$$

where $j_0$ is the flux of hydrogen atoms arriving the grain surface. The penetration of hydrogen in the grains results in a decreasing of hydrogen pressure registered by the TPA. Considering the molecular hydrogen gas as an ideal one, the number of hydrogen atoms is $N = 2pV/k_BT$, where $p$, $V$, and $T$ are pressure, volume, and temperature in the TPA, respectively. Because of $Aj_s = -\partial N/\partial t \propto -dp/dt$ ($A$ is the total surface area of grains) we obtain

$$\Delta p \propto -\Delta t \exp(-U_s/k_BT). \tag{8}$$

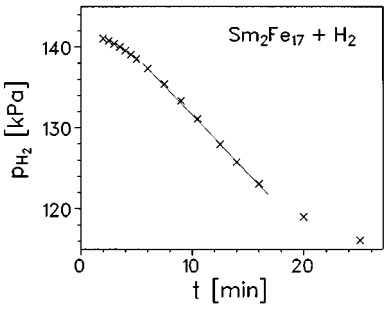


FIG. 7. Time dependence of pressure hydrogenating $Sm_2Fe_{17}$ at 200 °C in a surface controlled reaction. The linear decrease of pressure corresponds to Eq. (8).

A typical result for $T = 200\,^\circ$C (corresponding to a temperature in stage I of Fig. 2) is shown in Fig. 7. During heating, after a few minutes we find the expected linear decrease of pressure as a function of time. After 15 min the diffusion becomes slower and the linear variation eventually breaks down.

For determination of $U_s$, Eq. (8) can be written as

$$\ln\left(\frac{\Delta p}{m\Delta t}\right) = C - \frac{U_s}{k_BT}, \tag{9}$$

where $C$ is an unspecified constant and the surface area of the powdered material has been assumed to be proportional to its mass. Corresponding results in the temperature range 450–520 K are shown in Fig. 8, whence

$$U_s = 81(\pm 15)\ \text{kJ mole}^{-1}.$$

In comparison, for the $Nd(Fe_{11}Ti)$-hydrogen system a surface barrier $U_s = 59(\pm 15)$kJ mole$^{-1}$ has been found.

The surface barrier is not an intrinsic property of $R_2Fe_{17}$. It reflects the extent of contamination of the intermetallic surface. Such contamination of the particle surface could be due to $H_2O$ or OH, as discussed in Ref. 21.

### B. Bulk diffusion

In the case of spherical grains the diffusion Eq. (4) can be solved[36] (Fig. 9),

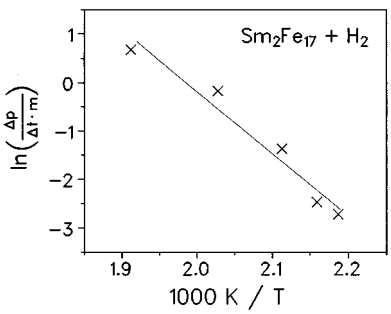


FIG. 8. Temperature dependence of normalized pressure decrease per time corresponding to Eq. (9) in the case of surface controlled absorption of hydrogen by $Sm_2Fe_{17}$.

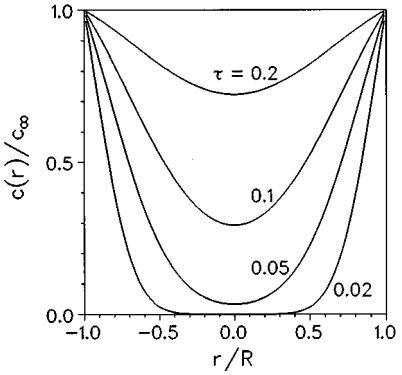


FIG. 9. Calculated concentration profile of diffusion controlled absorption using $\tau = Dt/R^2$.

$$c(r,t) = c_\infty \left( 1 + \frac{2R}{\pi r} \sum_{n=1}^{\infty} \frac{(-1)^n}{n} \sin \frac{n\pi r}{R} e^{-n^2\pi^2 Dt/R^2} \right), \tag{10}$$

where $c_\infty$ is the hydrogen concentration for $t \to \infty$. Integration over the grain volume yields

$$\frac{c(t)}{c_\infty} = 1 - \frac{6}{\pi} \sum_{m=1}^{\infty} \frac{1}{m^2} e^{-m^2\pi^2 Dt/R^2}. \tag{11}$$

The decrease of TPA pressure corresponds to an increase of concentration of hydrogen atoms in the bulk material, $c(t) \propto p_0 - p(t)$ and $c_\infty \propto p_0 - p_\infty$, where $p_0$ and $p_\infty$ represent the pressures for times $t = 0$ and $t = \infty$, respectively. Due to the high mobility of hydrogen only the first term of the sum in Eq. (11) needs to be considered and we obtain

$$\frac{p(t) - p_\infty}{p_0 - p_\infty} = \frac{\Delta p(t)}{\Delta p_0} = \frac{6}{\pi^2} e^{-\pi^2 Dt/R^2}. \tag{12}$$

The diffusion constant can be determined from a plot $\ln(\Delta p(t)/\Delta p_0)$ as a function of time, where a straight line is expected.

The temperature dependence of the diffusion constant is given by

$$D = D_0 e^{-U_a/k_B T}. \tag{13}$$

The activation energy $U_a$ as well as $D_0$ are obtained from the Arrhenius plot Fig. 4 resulting in $U_a = 31(\pm 10)$ kJ mol$^{-1}$ and $D_0 = 4.4 \times 10^{-7(\pm 2)}$ m$^2$ s$^{-1}$. The high error of $D_0$ is caused by the relatively small temperature region in which the diffusion experiments can be carried out. The agreement of the results of $Sm_2Fe_{17}H_x$ with given data[34] for $LaNi_5H_6$ can be explained by the similarity of the lattice structures. The diffusion values for $Sm_2Fe_{17}$ are substantially higher than in the tetragonal Nd($Fe_{11}$Ti) compound [$U_a = 45(\pm 12)$ kJ mol$^{-1}$, $D_0 = 5.8 \times 10^{-7(\pm 2)}$ m$^2$ s$^{-1}$]. A possible reason for this could be the lack of tetrahedral interstitial sites in the $ThMn_{12}$ structure (where only one octahedral 2*b* site per formula unit can be occupied by H). Hence the preferred diffusion paths of the 1:5 and 2:17 compounds are unavailable.

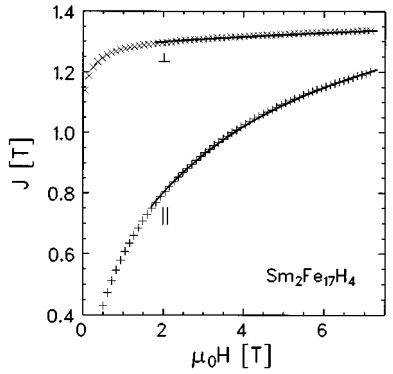


FIG. 10. Measured (markers, only every second data point is included) and calculated (lines) demagnetization curves of a $Sm_2Fe_{17}H_4$ sample with well-aligned grain *c* axes. The sample texture axis has been orientated parallel and perpendicular to the magnetic field, respectively.

## IV. MAGNETIC PROPERTIES OF $Sm_2Fe_{17}H_4$

For magnetic measurements, a sample was prepared from $Sm_2Fe_{17}$ powder (grain size $\leqslant 25$ $\mu$m) which was hydrided in the TPA for 3 h at 520 K. Under these conditions the hydrogen concentration should be nearly in equilibrium. From the pressure decrease inside the TPA the hydrogen content in $Sm_2Fe_{17}H_x$ has been determined as $x = 4.0$. A lattice expansion of $\Delta a/a = 1.3\%$, $\Delta c/c = 0.64\%$ and hence $\Delta V/V = 3.4\%$ after hydrogenation (2.3 Å$^3$/H) has been observed in agreement with data given in Ref. 37. A preferred alignment of the *c* axes of the particles was achieved by applying a rotating magnetic field of 0.6 T while the powder was set in epoxy resin.

Demagnetization curves of the $Sm_2Fe_{17}H_4$ sample measured with the sample texture axis parallel and perpendicular to the applied field are shown in Fig. 10. From a fit of the demagnetization curves[18] the anisotropy constants and the spontaneous polarization of the material have been determined, $K_1 = -4.2$ MJ m$^{-3}$, $K_2 = 0.6$ MJ m$^{-3}$, and $J_s = 1.34$ T, respectively, whereby the $K_i$ values correspond to the expected anisotropy of easy plane. Also, a texture parameter of the sample, $\sigma_g = 12.5°$, has been determined [a Gaussian-like texture function, $f(\alpha) \propto \exp(-\alpha^2/2\sigma_g^2)$, has been assumed where $\alpha$ is the orientation of the grains *c* axes with respect to the sample texture axis] confirming that a good crystallite alignment is achieved by the rotating field. In the fit procedure, reversible rotational processes of the magnetization of the differently oriented individual grains were taken into account and hence, the procedure is suitable for investigation of polycrystalline samples. The value obtained for $J_s$ is in agreement with those given elsewhere,[8,37] but the value of $K_1$ is significantly higher than that of Ref. 8. A maximum residual deviation between measured and fitted polarization values of less than 4 mT confirms the fit results. Note that polarization values measured at low fields are influenced by stray fields inside the sample and therefore, these were not taken into account in the fit procedure.

Starting from the anisotropy constants the parameters of the crystalline electric field (CEF) acting on the aspherical 4*f* electron shell of the rare-earth can be estimated.[38] The CEF is mainly caused by the interstitial H atoms on the

TABLE I. Saturation polarization $J_s$, anisotropy constants $K_1$ and $K_2$ and calculated CEF parameter $A_{20}$ at room temperature of $Sm_2Fe_{17}H_4$ compared with the parent compound and the nitride and carbide (Ref. 38).

| | $J_s$ (T) | $K_1$ ($MJ\,m^{-3}$) | $K_2$ | $A_{20}$ ($Ka_0^{-2}$) |
|---|---|---|---|---|
| $Sm_2Fe_{17}$ | 1.12 | −2.1 | 0.4 | 35 |
| $Sm_2Fe_{17}H_4$ | 1.34 | −4.2 | 0.6 | 110 |
| $Sm_2Fe_{17}C_{2.6}$ | 1.45 | 7.5 | 0.8 | −310 |
| $Sm_2Fe_{17}N_3$ | 1.54 | 9.1 | 1.6 | −400 |

octahedral sites surrounding the rare earth in a plane perpendicular to the crystallographic $c$ axis. This anisotropy is transferred to the 3$d$ electron system and hence to the magnetization via strong 4$f$-5$d$ $R$-Fe coupling and 5$d$-3$d$ hybridization. The results are $A_{20}\approx 110\ Ka_0^{-2}$ and $A_{40}\approx 42\ Ka_0^{-4}$. Here, the molecular field coefficient $n_{SmFe}=215$ has been estimated from the Curie temperatures of $Sm_2Fe_{17}H_x$ (554 K) and $Y_2Fe_{17}H_x$ (516 K) as described elsewhere.[39] Note that the value obtained for $n_{SmFe}$ depends sensitively on the Curie temperatures, e.g., using given data[40] would result in $n_{SmFe}=265$.

In Table I, the magnetic properties of $Sm_2Fe_{17}H_4$ at room temperature are compared with those[38] of $Sm_2Fe_{17}N_3$, $Sm_2Fe_{17}C_{2.6}$ and the parent $Sm_2Fe_{17}$ compound. Note that the increase of $J_s$ for the interstitially modified compounds is not only caused by the changed magnetic moment of the iron atoms[41] but mainly by the increased exchange coupling giving rise to the enhanced Curie temperature. Starting from the parent compound, the $A_{20}$ is changed in opposite directions by interstitial modification with H or N/C, respectively. According to Coehoorn and co-workers[42,43] we expect opposite trends in the change of the rare-earth valence electron density in the plane containing $R$ and interstitial atoms for H and N/C. Considering only relative electronegativity as in the screened charge model[44] our result shows the ''electropositive'' character of hydrogen whereas N and C are strongly electronegative.

## V. DISCUSSION

### A. Mobility

Hydrogen in metals generally shows a high mobility because its small atomic radius leads to comparatively small activation energies. The time $\tau$ which is necessary to overcome the potential barrier between two neighboring interstices can be estimated using

$$\tau=\tau_0\exp(-U_a/k_BT), \tag{14}$$

where $\tau_0^{-1}$ is the attempt frequency ($\tau\approx 10^{-13}$ s). At room temperature this yields times $\tau$ of about 1000 years in the case of nitrogen, but only $\tau\approx 10$ ms in the case of hydrogen. Whenever the measuring time is longer than about 10 ms, the experiment gives the impression that hydrogen is mobile at room temperature. This statement can be generalized to other metals, but often the hydrogen absorption is limited by the low equilibrium concentration, and the high diffusivity is less obvious.

### B. Diffusion mechanism, tunneling

Below some crossover temperature $T_0$, the leading diffusion mechanism is incoherent quantum tunneling.[45–47] For hydrogen, $T_0$ is of order 200 K, whereas the values for deuterium and tritium are much lower (isotope effect[46]). Following this rule, we should expect an even lower $T_0$ for other gases, such as nitrogen. This conclusion, however, is not quite correct. To estimate $T_0$ we use Eq. (14) and the semiempirical relation[36]

$$U_a=c_aEZ^{2/3}a_0^3, \tag{15}$$

where $c_a\approx 3$ is a numerical factor, $E$ is the elastic modulus, and $Z$ is the atomic number of the diffusing atom. The exponent 2/3 reflects the $R^2$ dependence of the ion energy, where $R\sim Z^{1/3}$ is the size of the diffusing atom.

To describe the quantum tunneling we use the following Gamov factor:

$$\tau'=\tau_0\exp\left(-\sqrt{\frac{8\,mU_a}{\hbar}}d\right), \tag{16}$$

where $d\sim 1$ Å is the thickness of the energy barrier. The tunneling time $\tau'$ is temperature independent, so at low temperatures, where thermal activation can be neglected, tunneling becomes the leading mechanism. Putting $\tau'=\tau$ we obtain the critical temperature

$$T_0=\sqrt{\frac{\hbar^2c_aEZ^{2/3}a_0^3}{8\,k_B^2md^2}}, \tag{17}$$

which is $T_0=170$ K for hydrogen in $Sm_2Fe_{17}$, and $T_0=90$ K for nitrogen in $Sm_2Fe_{17}$. Note that the nitrogen value is about two times higher than expected from the simple $1/\sqrt{m}$ isotope law.[46] Assuming $m\sim Z$ in Eq. (17) the surprising dependence $T_0\sim Z^{-1/6}$ is obtained.

This leads us to believe that below 77 K all interstitial atoms in question diffuse preferentially via quantum tunneling. Unfortunately, low-temperature measurements of D(N) are very difficult and no experimental values $T_0$(N) have been given thus far.

### C. Structure

X-ray investigations of $Sm_2Fe_{17}H_x$ prepared under equilibrium conditions did not show any evidence for phase segregation at above room temperature. However, because of the smaller lattice expansion (Fig. 1) such investigations are not as conclusive as in the case of $Sm_2Fe_{17}N_x$.[25]

As already described, equilibrium conditions are required for measurements of $U_0$, $U_a$, and $D_0$. For measurements at constant heating rate, the deviations from equilibrium can be seen from Fig. 2 ($Y_2Fe_{17}H_x$ sample). For temperatures below about 200 °C the hydrogen cannot be absorbed by the sample because of the surface barrier and the low diffusion constant. In a temperature region of about 270–340 °C the hydrogen cannot desorb as fast as the temperature increases (diffusion length $\sim 30\ \mu$m after 1 min at 270 °C, mean grain

size 40 $\mu$m). Only at higher temperatures is the equilibrium established. The different sites (tetrahedral and octahedral) complicate the determination of $U_{oct}$ and $U_{tet}$ in Eq. (2). However, a quantitative discussion is very difficult due to the possibility of gas absorption and desorption at the grain surface.

### D. Magnetic properties

The opposite trend in $A_{20}$ of the hydrided material compared to the nitride and carbide shows that different effects are involved in interstitial modification: changes of the spatial distances of the atoms/ions and changes of the electric charge distribution by the interstitial atoms and their hybridization with neighboring atoms (the hybridization of interstitially modified $R_2Fe_{17}$ is discussed, e.g., from *ab initio* calculations[43,48]). Since the host lattice always expands with interstitial modification the hybridization effect should be opposite in the hydrides compared with the N and C modification. A similar result was reported by Mössbauer spectroscopy of $Gd_2Fe_{17}H_x$.[49]

## VI. CONCLUSIONS

Iron-rich rare-earth intermetallics such as $Sm_2Fe_{17}$ can absorb large quantities of hydrogen. Intermediate hydrogen concentration indicate a more or less ideal solid solution with net reaction energies of $26(\pm 4)$ kJ mole$^{-1}$ for the octahedral sites in $Sm_2Fe_{17}$. The gas-solid reaction rate is determined by bulk diffusion (above about 350 °C) whereas at lower temperatures the particle flux is limited by surface energy barriers of $81(\pm 15)$ kJ mole$^{-1}$. The bulk diffusion constant of $4.4\times 10^{-7(\pm 2)}$ m$^2$ s$^{-1}$ and activation energy of $31(\pm 10)$ kJ mole$^{-1}$ are typical for intermetallic compounds.

An estimation of the transition temperature between thermally activated diffusion and quantum tunneling yields that quantum tunneling dominates below about 170 K for hydrogen and 90 K for nitrogen. It would be interesting to confirm this prediction experimentally.

The effect of hydrogen interstitial modification of $Sm_2Fe_{17}$ on the magnetocrystalline anisotropy is shown to be opposite to N and C. The hydrogen does not provide useful, easy-axis anisotropy in $Sm_2Fe_{17}$, but there is a possibility that it could be used for rare earths such as Nd or Dy which have a negative Stevens coefficient $\alpha_J$.

## ACKNOWLEDGMENTS

The authors are grateful to Dr. Hong Sun for help in experimental details. This work formed part of the CEAM program of the EC. S.W. has been financially supported by CEAM–HCM.

*Present address: IFW Dresden, P.O. 270016, 01171 Dresden, Germany.

†Present address: MPI for Microstructural Physics, Halle, Germany.

[1] T. Graham, Philos. Trans. R. Soc. **156**, 399 (1866).
[2] K. H. J. Buschow, Rep. Prog. Phys. **54**, 1123 (1991).
[3] H. H. van Mal, K. H. J. Buschow, and A. R. Miedema, J. Less-Common Met. **42**, 65 (1975).
[4] X.-Z. Wang, K. Donnelly, J. M. D. Coey, B. Chevalier, J. Etourneau, and T. Berlureau, J. Mater. Sci. **23**, 329 (1988).
[5] Hu Bo-ping and J. M. D. Coey, J. Less-Common Met. **142**, 295 (1988).
[6] J. M. D. Coey and Hong Sun, J. Magn. Magn. Mater. **87**, L251 (1990).
[7] O. Isnard, J. L. Soubeyroux, S. Miraglia, D. Fruchart, L. M. Garcia, and J. Bartolomé, Physica B **180–181**, 629 (1992).
[8] O. Isnard, S. Miraglia, M. Guillot, D. Fruchart, and K. H. J. Buschow, J. Appl. Phys. **76**, 6035 (1994).
[9] K. Yvon and P. Fischer, in *Hydrogen in Intermetallic Compounds I*, edited by L. Schlapbach (Springer-Verlag, Berlin, 1988), p. 87.
[10] J. D. Fast, *Gases in Metals* (Macmillan, London, 1976).
[11] F. Spada and H. Oesterreicher, J. Less-Common Met. **107**, 301 (1985).
[12] H. Wagner and H. Horner, Adv. Phys. **23**, 587 (1974).
[13] H. Peisl, in *Hydrogen in Metals I*, edited by G. Alefeld and J. Völkl (Springer, Berlin, 1978), p. 53.
[14] M. Katter, J. Wecker, L. Schultz, and R. Grössinger, J. Magn. Magn. Mater. **92**, L14 (1990).
[15] D. Fruchart and S. Miraglia, J. Appl. Phys. **68**, 5578 (1991).
[16] Ying-chang Yang, Xiao-dong Zhang, Lin-shu Kong, Qi Pan, and Sen-li Ge, Appl. Phys. Lett. **58**, 2042 (1991).
[17] X. C. Kou, R. Grössinger, M. Katter, J. Wecker, L. Schultz, T. H. Jacobs, and K. H. J. Buschow, J. Appl. Phys. **70**, 2272 (1991).
[18] K.-H. Müller, D. Eckert, P. A. P. Wendhausen, A. Handstein, S. Wirth, and M. Wolf, IEEE Trans. Magn. **30**, 586 (1994).
[19] D. Fruchart, O. Isnard, S. Miraglia, and J.-L. Soubeyroux, J. Alloys Compd. **231**, 188 (1995).
[20] D. H. Ryan and J. M. D. Coey, J. Phys. E **19**, 693 (1986).
[21] C. Murray, N. Dempsey, and J. M. D. Coey, J. Alloys Compd. **215**, 345 (1994).
[22] T. Takeshita, J. Alloys Compd. **193**, 231 (1993).
[23] H. Zabel and H. Peisl, Phys. Rev. Lett. **42**, 511 (1979).
[24] H. Zabel and H. Peisl, J. Phys. F **9** 1461 (1979).
[25] J. M. D. Coey, R. Skomski, and S. Wirth, IEEE Trans. Magn. **28**, 2332 (1992).
[26] M. Katter, J. Wecker, C. Kurth, L. Schultz, and R. Grössinger, J. Magn. Magn. Mater. **117**, 419 (1992).
[27] C. N. Christodoulou and T. Takeshita, J. Alloys Compd. **202**, 173 (1993).
[28] J. D. Eshelby, Acta Metall. **3**, 487 (1955).
[29] H. Wagner, in *Hydrogen in Metals I*, edited by G. Alefeld and J. Völkl (Springer, Berlin, 1978), p. 5.
[30] M. Brouha and K. H. J. Buschow, J. Appl. Phys. **44**, 1813 (1973).
[31] J. P. Gavigan, D. Givord, H.-S. Li, and J. Voiron, Physica **B 149**, 349 (1988).
[32] R. Skomski, S. Brennan, and S. Wirth, in *Interstitial Intermetallic Alloys*, edited by F. Grandjean, G. J. Long, and K. H. J. Buschow (Kluwer, Dortrecht, 1995), p. 371.
[33] Y. Fukai, *The Metal-Hydrogen System* (Springer-Verlag, Berlin, 1993).
[34] R. Hempelmann, J. Less-Common Met. **101**, 69 (1984).
[35] R. Kutner, K. Binder, and K. W. Kehr, Phys. Rev. B **26**, 2967 (1982).
[36] B. S. Bokštein, *Diffusion in Metals* (Russian) (Metallurgija, Moscow, 1978).

[37] C. N. Christodoulou and T. Takeshita, J. Alloys Compd. **194**, 113 (1993).
[38] S. Wirth, M. Wolf, K.-H. Müller, R. Skomski, S. Brennan, and J. M. D. Coey, IEEE Trans. Magn. **32**, 4746 (1996).
[39] E. Belorizky, M. A. Fremy, J. P. Gavigan, D. Givord, and H. S. Li, J. Appl. Phys. **67**, 3971 (1987).
[40] O. Isnard, S. Miraglia, J. L. Soubeyroux, D. Fruchart, and P. l'Héritier, J. Magn. Magn. Mater. **137**, 151 (1994).
[41] G. Wiesinger and G. Hilscher, in *Handbook of Magnetic Materials VI*, edited by K. H. J. Buschow (Elsevier, Amsterdam, 1991), p. 511.
[42] R. Coehoorn, in *Supermagnets, Hard Magnetic Materials*, edited by G. J. Long and F. Grandjean (Kluwer, Dortrecht, 1991), p. 133.
[43] R. Coehoorn and G. H. O. Daalderop, J. Magn. Magn. Mater. **104-107**, 1081 (1992).
[44] R. Skomski, Philos. Mag. B **70**, 175 (1994).
[45] K. W. Kehr, in *Hydrogen in Metals I*, edited by G. Alefeld and J. Völkl (Springer, Berlin, 1978), p. 197.
[46] L. L. Dhawan and S. Prakash, J. Phys. F **14**, 2329 (1984).
[47] Zh. Qi, J. Völkl, R. Lässer, and H. Wenzel, J. Phys. F **13**, 2053 (1983).
[48] T. Beuerle and M. Fähnle, Phys. Status Solidi B **174**, 257 (1992).
[49] O. Isnard, P. Vulliet, A. Blaise, J. P. Sanchez, S. Miraglia, and D. Fruchart, J. Magn. Magn. Mater. **131**, 83 (1994).